LIMNOLOGY
AND
OCEANOGRAPHY

January 1996
Volume 41
Number 1

Limnol. Oceanogr., 41(1), 1996, 1–15

A dynamic model of photoadaptation in phytoplankton

Richard J. Geider[1] *and Hugh L. MacIntyre*
Graduate College of Marine Studies, University of Delaware, Lewes 19958-1298

Todd M. Kana
Horn Point Environmental Laboratories, University of Maryland, Cambridge 21613-0775

Abstract

We present a new dynamic model that uses a small number of prescribed parameters to predict the chlorophyll *a*:carbon ratio and growth rate of phytoplankton in both constant and varying irradiance. The model provides a self-contained description of energy and mass fluxes and regulation of partitioning of photosynthate during phytoplankton adaptation to irradiance. The kinetics and steady-state outcomes of photoadaptation are described in terms of changes in the rates of synthesis of three intracellular carbon pools. These pools account for the distribution of cell material between light-harvesting components, the biosynthetic apparatus, and energy storage compounds. Regulation of the flow of recent photosynthate to these pools is controlled by the ratio of realized to potential photosynthetic electron flow at a given instant. The responses of growth rate and Chl *a*:C to static and dynamic irradiance regimes can be adequately described by specifying four parameters: the initial slope of the photosynthesis-irradiance curve, the maximum growth rate, the maximum Chl *a*:C observed under light limitation, and the maintenance metabolic rate. The model predictions compared favorably with observations of the diatoms *Thalassiosira pseudonana* and *Phaedactylum tricornutum*.

Photoadaptation, involving the down-regulation of pigment synthesis at high irradiance, is well documented in procaryotic and eucaryotic phytoplankton (Falkowski and La Roche 1991). The chlorophyll *a* : carbon ratio (θ) and the chlorophyll *a*-specific light-saturated photosynthesis rate (P^{Chl}_m) are two of the most widely used indices of the photoadaptive state of phytoplankton (Geider 1993). θ provides a link between phytoplankton growth rate (μ) and the commonly measured chlorophyll *a*-specific photosynthesis rate P^{Chl} (i.e. $\mu = P^{Chl}\,\theta$) (Eppley 1972). Since chlorophyll *a* is the most widespread index of phytoplankton abundance (Cullen 1982), photoadaptation of θ and P^{Chl} has significant implications for our understanding of phytoplankton ecology and biooptical modeling of primary productivity. Variability in θ can lead to considerable uncertainty in both the biomass and specific growth rate of phytoplankton. Finally, our understanding of particle dynamics in the upper ocean rests on our ability to describe and predict θ and P^{Chl}.

Oceanographers and limnologists have made significant progress in modeling balanced phytoplankton growth quantitatively. The models have a common basis in depicting phytoplankton growth in terms of mass and energy fluxes (Geider 1993; Cullen et al. 1993) that describe light absorption and carbon assimilation for a cell with a specified light-harvesting composition (i.e. θ). Despite the success of these models in providing an internally consistent description of phytoplankton growth, photosynthesis, and pigment content (Sakshaug et al. 1989), they are little more than accounting procedures because they cannot be used to simultaneously predict the light dependencies of both θ and μ. Specifically, the prediction of the light dependence of μ requires specification of the light dependence of θ. Alternatively, prediction of the light dependence of θ requires specification of the light dependence

[1] To whom correspondence should be addressed. Present address: Marine Biological Association of the U.K., The Laboratory, Citadel Hill, Plymouth PL1 2PB, England.

Acknowledgments

We acknowledge support from NSF grants OCE 93-01768 (R.J.G.) and OCE 93-05896 (T.M.K.) and DOE DE-FG02-93ER6195 (R.J.G.).

We thank John Cullen for a thought-provoking review and Paul Falkowski for providing preprints of works in press. We also thank Peggy Conlon for assistance in preparing the manuscript.

Contribution 2663 from the Center for Environmental and Estuaries Studies of the University of Maryland System.

of μ. This circularity reduces the predictive power of these models of balanced growth. In this paper, we relax this constraint by imposing biological regulatory rules that govern changes in the photosynthetic apparatus and distribution of cell materials in response to irradiance. This approach provides a method for describing both steady-state (i.e. constant irradiance) and dynamic (i.e. fluctuating irradiance) responses in a unified conceptual framework and can thus be used in the context of real-world effects on phytoplankton exposed to changing light fields. Additionally, the formulation and testing of the regulatory rules can provide insight into the regulation of photosynthesis in diverse taxa.

Photoadaptive responses have been observed in stably stratified water columns (Harrison and Platt 1986) and following manipulations of samples taken from the surface mixed layer (Lewis et al. 1984*b*). Investigations of bio-optical properties of particulate matter (Mitchell and Kiefer 1988) and single cell pigment content that use flow cytometery (Li et al. 1993) have demonstrated adaptation of pigment content in natural phytoplankton populations. However, the significance of photoadaptation in regulating the rate of primary productivity in the sea has been difficult to evaluate because irradiance fluctuates over a wide range of time scales that cannot be adequately mimicked by conventional experimental techniques. Although vertical mixing has been shown to modulate primary productivity (Marra 1978; Gallegoes and Platt 1985), evaluating the quantitative significance of vertical mixing in nature requires explicit models incorporating a description of physical mixing and physiological responses (Kamykowski et al. 1994). Many of these models have focused on photosynthetic responses that occur on the relatively short time scales of minutes to hours. Photoadaptation of pigment content on the longer time scales of hours to days is associated with cell growth and division and is also likely to be important. It is this latter scale of response that is the subject of our dynamic model of photoadaptation.

Photoadaptation kinetics are typically modeled with empirically determined first-order rate constants, although expressions other than first-order rate equations may be more appropriate (Cullen and Lewis 1988). Geider and Platt (1986) provided a mechanistic basis for establishing the first-order rate constants for photoadaptation from mass budgets for cell carbon and Chl *a*. They showed that the first-order description was a special case of a more general behavior. Cullen and Lewis (1988) have compared various formulations of the kinetics of photoadaptation. In this paper, we describe a dynamic model of phytoplankton growth and photoadaptation under nutrient-replete conditions that extends the analysis of Geider and Platt (1986). The key feature of the model is an explicit description of the regulation of the biosynthesis of light-harvesting pigments by the ratio of photosynthesis to light harvesting. One can think of this ratio as a measure of the oxidation-reduction status of the photosynthetic electron transfer chain. The model shows how photoadaptation can arise out of the dynamics of partitioning of carbon among intracellular pools and specifies both balanced growth and transient responses to changes of irradiance. The model is unique in that the same parameters that determine μ and θ in balanced growth also predict the transients that occur following changes of irradiance.

Theory: A dynamic model of phytoplankton growth and photoadaptation

For simplicity, we assume that cellular macromolecules fall into one of three categories: pigments and proteins whose abundances are light regulated, macromolecules whose abundances are not light regulated, and energy reserve carbohydrates and lipids. To the best of our knowledge, there is no single data set that allows the light dependencies of all three of these classes of cell components to be illustrated for an alga. However, it is possible to provide examples of the different light dependencies of these three classes of macromolecules by combining data from several sources (Fig. 1). The down-regulation of light-harvesting components as irradiance increases is illustrated by the light dependence of several components of the thylakoid membranes in *Dunaliella tertiolecta* (Fig. 1B). Under low light conditions, the sum of pigments, light-harvesting complex 2, and electron transport chain proteins and associated lipids can equal 30% of cell carbon in *D. tertiolecta*. Examples of catalysts whose abundances are not light regulated are provided by RNA in *Thalassiosira weisflogii* (Fig. 1C), the Calvin cycle enzyme Rubisco (ribulose 1,5-bisphosphate carboxylase-oxygenase) in *D. tertiolecta* (Fig. 1B), and residual carbohydrates in *Thalassiosira pseudonana* (Fig. 1A). Finally, an example of the dependence of energy reserve polymers on growth irradiance is provided by the increase of hot-water-extractable carbohydrates with increasing irradiance in *T. pseudonana* (Fig. 1A).

Like the models of Shuter (1979) and Lancelot et al. (1991), our model considers the phytoplankton cell to consist of a number of functional, structural, and storage pools. Our model is based on the flow of carbon to three intracellular pools (Fig. 2). It combines the treatment of energy and mass fluxes (i.e. photon absorption and changing pool sizes) with the description of regulation (i.e. signal transduction and regulation of biosynthesis). Significantly, the model is formulated in such a way that photoadaptation is regulated by the energy and mass fluxes. Thus, the model is self-contained, with energy-mass fluxes providing the information that regulates the synthesis of the components that catalyze these fluxes.

Intracellular carbon is distributed among the light-harvesting apparatus (designated L), the biosynthetic apparatus (designated E), and an energy storage reserve (designated R). Although abstractions, these pools can be associated with fundamental aspects of energy transduction and storage (Fig. 1). L consists of the photosynthetic pigment-protein complexes and supporting membranes, together with the reaction centers and electron transfer chain. In the jargon of photosynthetic units, we assume constant photosynthetic unit composition and stoichiometry (i.e.

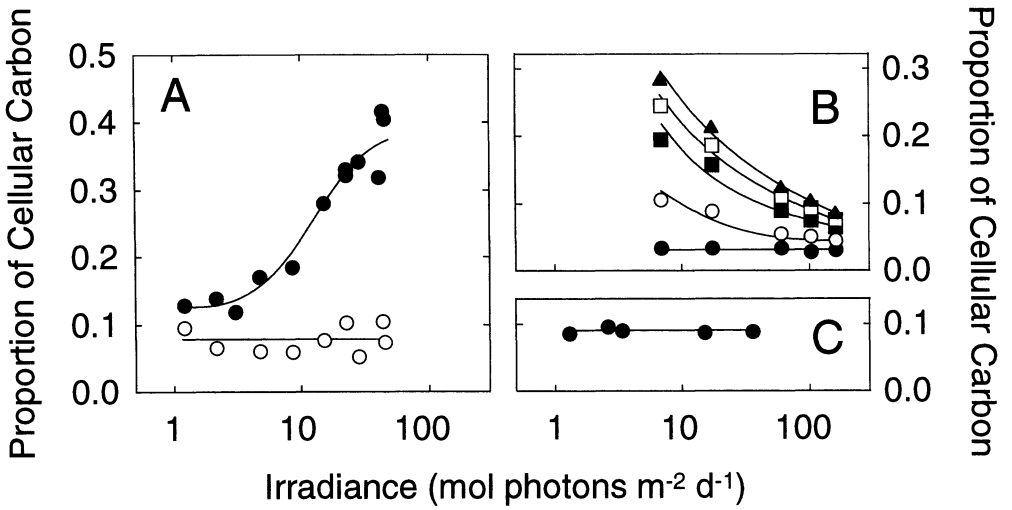

Fig. 1. Variation of biochemical composition with growth irradiance in microalgae illustrating light-regulated components, light-independent components, and storage components. A. Proportion of cell C accounted for by total (●) and residual (○) carbohydrates in *Thalassiosira pseudonana* (Geider 1984). The difference between total and residual carbohydrates is attributable to hot-water-extractable energy reserve polymers. Carbohydrates are assumed to be 40% C by weight. B. Cumulative proportion of cell C in Rubisco and thylakoid membrane components of *Dunaliella tertiolecta*. Rubisco (●) plus pigments (○) plus light-harvesting complex 2 proteins (■) plus photosynthetic electron transfer chain components (□) plus thylakoid lipids (▲). The sum of these components (▲) underestimates the total C in thylakoid membranes because it does not include contributions from light-harvesting complex 1 components, the ATP synthase complex, and mobile electron carriers. Cellular concentrations of Rubisco, photosynthetic pigments, and light-harvesting complex 2 proteins were obtained from Sukenik et al. (1987). Rubisco is assumed to have a molecular weight of 560 kDa (Miziorko and Lorimer 1983), 50% of which is attributed to C. Photosynthetic electron transfer system components were calculated from photosystem 1, photosystem 2, and cytochrome b_6/f concentrations reported by Sukenik et al. (1987) and the following molecular weights for the thylakoid membrane complexes: 280 kDa for the photosystem 2 complex (Erickson and Rouchaix 1992), 98 kDa for the cytochrome b_6/f complex (Hope 1993), and 280 kDa for the PS1 complex (Ikeuchi 1992). Protein is assumed to be 50% C by weight. Thylakoid membrane lipid is assumed to equal 19% of protein in the integral membrane complexes (Raven 1984), and lipid is 74% C by weight. *D. tertiolecta* is assumed to have a cell C content of 29 pg $cell^{-1}$, independent of irradiance (Falkowski and Owens 1980). C. Proportion of cell C in RNA of *Thalassiosira weisflogii*. RNA:C ratios for *T. weisflogii* (mean of 0.15 gRNA g^{-1} C) were obtained from Laws et al. (1983). The amount of cell C associated with RNA was calculated as 59% of the RNA:C ratio based on the assumptions that RNA is 35% C by weight, that ribosomes account for 90% of cellular RNA, and that ribosomes are 35% protein and 65% RNA by weight (Whittmann 1982).

a constant ratio of pigments to reaction centers 1 and 2 and photosynthetic electron transfer chain components). We do not consider possible changes of pigment-protein composition and photosynthetic unit size (Falkowski and La Roche 1991) that may be observed in phytoplankton. E can be considered to consist of the enzymes involved in carbon fixation and in the elaboration of fixed carbon into new cells. E thus includes the machinery of biosynthesis and cell replication. It also includes the Calvin cycle enzyme, Rubisco, which does not seem to be light regulated in chlorophytes (Sukenik et al. 1987; Fisher et al. 1989; *but see* Orellana and Perry 1992 for an example of light regulation of Rubisco content in a diatom). R is considered to consist of those polysaccharides and lipids that serve as energy storage reserves.

The present model of photoadaptation is strictly applicable to photoadaptation only under nutrient-sufficient conditions. In addition, we limit our description of model behavior to changes of Chl *a* and particulate organic C because these are the variables for which data are most readily available. It will be possible to evaluate more elaborate models with increased availability of quantitative data on the concentrations of photosynthetic proteins (including Rubisco, light-harvesting complex proteins, and electron transfer chain proteins) and other macromolecules or macromolecular assemblages, such as ribosomal RNA. For the present, we must be content with the more limited description of changes in Chl *a* and C that the available database can support. However, even this primitive description of phytoplankton photosynthesis provides insights into photoadaptation, phytoplankton growth, and productivity.

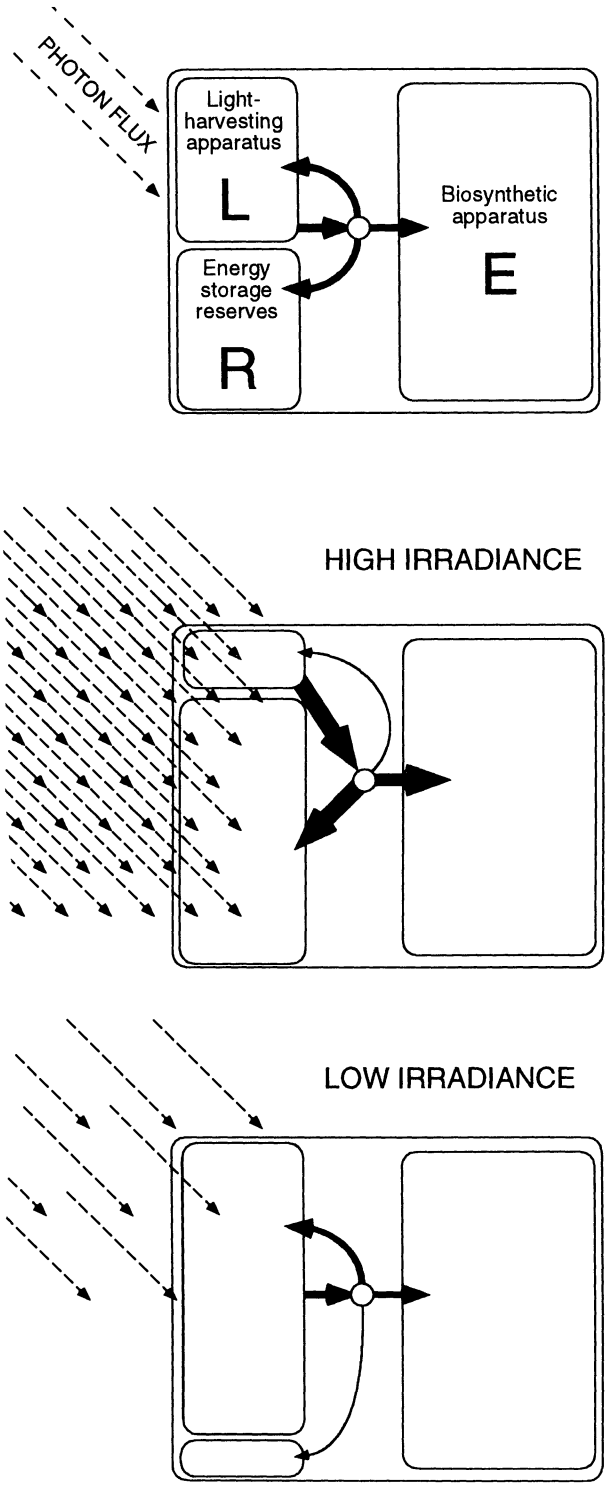

Fig. 2. Diagrammatic representation of the dynamic model of phytoplankton growth and photoadaptation. The three intracellular pools are identified in the top panel. The solid arrows and circle in the upper panel illustrate the flux of excitation energy into a control point and of photosynthate out of the control point. The middle panel illustrates the small size of L and the large size of R in high light-adapted cells. The solid arrows illustrate the high flux of excitation energy into the control point and allocation of photosynthate among the intracellular pools. The bottom panel illustrates the large size of L and small size of R in low light-adapted cells. The flux of excitation energy into the control point is markedly reduced relative to high light-adapted cells. The proportion of photosynthate allocated to synthesis of L is greater in low light-adapted cells, although the absolute amount may actually be smaller because of light limitation of photosynthesis.

The link between photon flux and mass flux is provided by the photosynthesis-irradiance (*PI*) curve (Eq. 1). Note that the rate of photosynthesis is expressed relative to the C content of the biosynthetic pool and is designated P^E, where the superscript E refers to the biosynthetic apparatus. (A list of notation is provided.)

$$P^E = P^E_m\left[1 - \exp\left(\frac{-\sigma I L}{P^E_m E}\right)\right]. \quad (1)$$

I is irradiance, E the C content of the biosynthetic apparatus, L the C content of the light-harvesting apparatus, P^E the rate of C fixation normalized to the size of the biosynthetic apparatus, P^E_m the maximum value of P^E, and σ the functional cross-section of the light-harvesting apparatus. σ can also be considered the L-specific initial slope of the *PI* curve, operationally defined as the product of the Chl *a*-specific light absorption coefficient (designated a^*_{Chl}), the maximum quantum efficiency for photosynthesis (designated ϕ_m), and the ratio of Chl *a* to C in L (Chl *a*: L). We make the simplifying assumption that σ, P^E_m, and Chl *a*: L are independent of growth irradiance, which is broadly consistent with observations (Geider 1993). As formulated here, the model applies only to constant temperature. However, temperature dependence can be readily incorporated into the model (Geider et al. in prep.) through specification of the temperature dependence of P^E_m, assuming also that a^*_{Chl} and ϕ_m are independent of temperature (*but see* Raven and Geider 1988).

Note that the rate of C fixation (Eq. 1) is determined by size of both the biosynthetic (E) and light-harvesting (L) pools. The relative importance of each pool in controlling the rate of C fixation depends on irradiance. Light-limited photosynthesis is controlled by L, but light-saturated photosynthesis is controlled by E. Both pools are important in the transition from light limitation to light saturation. The L : E ratio varies as a consequence of photoadaptation (Fig. 2), and thus the photoadaptive state of the phytoplankton is explicit in Eq. 1.

We assume that recent photosynthate can have three fates (Fig. 2). It can be used in the synthesis of new L, E, or R. The net rate of synthesis of L, E, or R is determined by the difference between production and degradation as follows:

$$\frac{dL}{dt} = \rho_L P^E E - r_m L, \quad (2)$$

$$\frac{dE}{dt} = \rho_E P^E E - r_m E, \quad (3)$$

Notation

I	Irradiance, mol photons m^{-2} d^{-1}
E	Biomass of the biosynthetic machinery, g C m^{-3}
L	Biomass of the photosynthetic apparatus, g C m^{-3}
R	Biomass of the storage pool, g C m^{-3}
α	Initial slope of the *PI* curve, g C (mol^{-1} photons) m^2 g^{-1} Chl *a*
θ	Chl *a*:C, g Chl g^{-1} C
Chl:L	θ in the photosynthetic apparatus, g Chl g^{-1} C
P^{C}_{m}	Maximum C-specific rate of photosynthesis, d^{-1}
P^{E}	E-specific rate of photosynthesis, d^{-1}
P^{E}_{m}	Maximum E-specific rate of photosynthesis, d^{-1}
a^{*}_{Chl}	Chl *a*-specific light absorption coefficient, m^2 g^{-1} Chl *a*
r_m	Maintenance metabolic coefficient, d^{-1}
σ	Functional cross-section of the L, m^2 mol^{-1} photons
κ_L	Maximum proportion of biosynthate allocated to synthesis of L, dimensionless
κ_E	Proportion of biosynthate allocated to synthesis of E, dimensionless
k_L	Maximum rate of M_L synthesis, d^{-1}
k_E	Maximum rate of M_E synthesis, d^{-1}
k_t	Time constant for M_L, M_E, and M_R degradation, d^{-1}
ρ_L	Proportion of photosynthate allocated to synthesis of L, dimensionless
ρ_E	Proportion of photosynthate allocated to synthesis of E, dimensionless
ρ_R	Proportion of photosynthate allocated to synthesis of R, dimensionless
M_L	Signal coding for L synthesis, relative units
M_E	Signal coding for E synthesis, relative units
M_R	Signal coding for R synthesis, relative units
M_T	Sum of $M_L + M_E + M_R$, relative units

and

$$\frac{dR}{dt} = \rho_R P^E E - r_m R. \quad (4)$$

ρ_L, ρ_E, and ρ_R designate the proportions of photosynthate directed to synthesis of L, E, and R. The degradation of all three pools is described by a first-order rate process governed by the parameter r_m. We have assumed that r_m is the same for all three classes of macromolecule and that it is independent of growth rate.

These simplifying assumptions can be criticized on several grounds. Dark respiration is typically linearly related to growth rate in algae, although the slope of a regression of respiration rate on growth rate can vary by a factor of five among species (Geider 1992). Dark respiration is likely to continue in the light, although whether it continues at rates greater than, less than, or equal to the rate of darkness is a matter of contention (Geider 1992). In addition, turnover of carbohydrate energy reserves may occur at much faster rates than turnover of pigments and proteins. A more realistic description of the relationship between biosynthesis and respiration would require that we specify additional parameters that are largely unconstrained by available data. Although we could have incorporated more realistic descriptions of respiration into the model, we have found that the solution of the model for conditions of balanced growth is largely unaffected by reasonable descriptions of the interdependence of biosynthesis and respiration (Geider et al. in prep.). We consider some of the limitations of our parameterization of respiration during the transient conditions following changes of irradiance in the discussion.

A key component in developing a dynamic model of photoadaptation is to specify the rules used by a cell to allocate recent photosynthate among the intracellular pools. Regulation enters the model through the specification of ρ_L, ρ_E, and ρ_R. We assume that the reduction state of a component of the photosynthetic electron transfer chain acts as a signal controlling allocation of photosynthate (Escoubas et al. 1995). We arbitrarily parameterize this signal by the ratio of C fixation to light harvesting [i.e. $(P^E E)/(\sigma I L)$]. We will judge the success of this parameterization by the fit of the model to observations. Note that $(P^E E)/(\sigma I L)$ equals the ratio of realized to maximum quantum efficiency of photosynthesis and is related to the rate of electron transfer to NADPH relative to the rate of photon supply to the photosynthetic apparatus. This ratio can also be viewed as a balance point around which the cell adjusts its light harvesting to match its ability to utilize photosynthate (Kana and Glibert 1987). This ratio decreases during a shift-up in light, providing a cue for down-regulating synthesis of L. A biological basis for this ratio is found in the regulation of an energy balance within the light reactions of photosynthesis and will be discussed more fully elsewhere (Kana et al. in prep.).

We specify ρ_L, ρ_E, and ρ_R as follows:

$$\rho_L = \kappa_L \frac{P^E E}{\sigma I L}; \qquad \rho_E = \kappa_E; \qquad \rho_R = \kappa_L \left(1 - \frac{P^E E}{\sigma I L}\right). \quad (5)$$

κ_L is the maximum proportion of photosynthate directed to synthesis of the light-harvesting component, and κ_E is the constant proportion of photosynthate directed to synthesis of the biosynthetic apparatus. Both κ_L and κ_E are dimensionless coefficients, and conservation of mass re-

quires that $\kappa_L + \kappa_E = 1.0$. The rate of change of the total phytoplankton carbon pool is given by the sum of the rates of change of the three intracellular pools in Eq. 6:

$$\frac{dC}{dt} = \frac{dL}{dt} + \frac{dE}{dt} + \frac{dR}{dt} = P^E E - r_m C. \quad (6)$$

Equations 2 and 5 set the rate of synthesis of L equal to the product of three terms: the maximum proportion of photsynthate devoted to synthesis of L at limiting irradiance (designated κ_L), the rate of photosynthesis (given by $P^E E$), and the regulatory parameter $(P^E E)/\sigma I L$). Since the ratio $(P^E E) : (\sigma I L)$ decreases as irradiance is raised, the model requires down-regulation of the synthesis of L relative to synthesis of E at high light. Equations 3 and 5 set the rate of flow of recent photosynthate to E to a constant proportion (κ_E) of the instantaneous rate of photosynthesis. Thus, the proportion of photosynthate allocated to synthesis of E is independent of irradiance (i.e. E is not light regulated), although the absolute rate of synthesis of E depends on irradiance through the *PI* curve (Eq. 1). Equations 4 and 5 specify that R increases in size only when photosynthate is diverted away from synthesis of L (thus, $\rho_L + \rho_R = \kappa_L$). In other words, photosynthate is increasingly directed to storage as the instantaneous rate of photosynthesis approaches light saturation (Fig. 2), consistent with observations (Morris 1981; Li and Platt 1982). Photoadaptation occurs through variations in ratio L : E, with synthesis of L down-regulated relative to synthesis of E as irradiance increases. Inspection of Eq. 2 and 5 shows that the maximum size of L is obtained as irradiance approaches zero and is given by $L/C = \kappa_L$. The upper limit on the size of R is achieved as irradiance becomes very large and approaches the limit $R/C = \kappa_L$.

The storage pool should be capable of supporting continued flow of carbon to both E and L in the event that photosynthesis declines due to a reduction of irradiance. Accumulation of carbohydrates during the day and mobilization at night have been reported for several algae and cyanobacteria (Foy and Smith 1980; Cuhel et al. 1984; Lancelot and Mathot 1985). In addition, carbohydrates may be preferentially respired during the day (Li and Harrison 1982; Lancelot and Mathot 1985). In contrast to these observations, we have assumed that the energy reserve pool is not preferentially mobilized in order to avoid making ad hoc assumptions regarding the parameterization of mobilization of energy reserve products. Despite this limitation, the model provides a robust description of photoadaptation, indicating that the regulatory term $(P^E E)/(\sigma I L)$ captures an essential feature of phytoplankton photophysiology.

The model (Eq. 2–4) requires that we specify four parameters σ, P^E_m, κ_L, and r_m. σ is the light absorption cross-section for L; P^E_m is the maximum rate of photosynthesis normalized to the size of the biosynthetic pool; κ_L gives the maximum proportion of photosynthate that can be directed to synthesis of L; r_m is the maintenance metabolic rate. Note that the proportion of photosynthate directed toward synthesis of E is given by $\kappa_E = 1 - \kappa_L$. Given values for the four parameters, the model predicts the time-dependent evolution of the sizes of L, E, and R. The allocation of photosynthate among these pools is regulated by the ratio $(P^E E) : (\sigma I L)$, which determines the realized and potential fluxes of photons, electrons, and carbon through the cell. We now turn to an evaluation of the numerical values of these four parameters and then to the application of the model to balanced growth in the diatoms *Phaeodactylum tricornutum* and *T. pseudonana.*

Selection of parameter values

The light absorption cross-section—σ is related to the Chl *a*-specific initial slope of the *PI* curve through Eq. 7:

$$\sigma = \alpha \text{ Chl} : L = a^*_{\text{Chl}} \phi_m \text{ Chl} : \text{L}. \quad (7)$$

α is the initial slope of the *PI* curve and Chl : L is the ratio of Chl *a* to C in the photosynthetic machinery. We have chosen a value for α of 10. The value is consistent with a typical maximum quantum efficiency for photosynthesis of $\phi_m = 0.083$ mol C mol^{-1} photons and typical in vivo light absorption coefficient of $a^*_{\text{Chl}} = 10$ m^2 g^{-1} Chl *a* (Langdon 1988; Geider 1993). It remains to estimate the Chl *a* : C ratio of the photosynthetic apparatus (Chl : L). There is conflicting evidence on this ratio. Raven (1984) calculated a Chl *a* : C ratio for the thylakoid membranes of 0.33. In contrast, Friedman and Alberte (1984) and Owens and Wold (1986) present data that suggests a much lower ratio of 0.10–0.15 for the thylakoid membranes of *P. tricornutum.* However, it is difficult to reconcile these lower ratios with the observed maximum Chl *a* : C ratio (θ_{max}) of 0.08 for whole cells (Geider et al. 1986; Cullen and Lewis 1988). We have chosen a value of Chl : L = 0.2, although we recognize that this value is subject to considerable uncertainty and is deserving of further measurements. Given α = 10 g C (mol^{-1} photons) m^2 (g^{-1} Chl *a*) and Chl : L = 0.2, we calculate that $\sigma = \alpha$ Chl : L = 2.0 m^2 mol^{-1} photons.

Proportion of photosynthate directed to synthesis of L—In the limit as irradiance approaches zero, Chl *a* : C approaches a maximum value (θ_{max}) (Geider 1987). In this limit, the ratio of L to C is given by the dimensionless constant, κ_L. Using a value of $\theta_{max} = 0.08$ obtained under extreme light limitation in *P. tricornutum* (Geider et al. 1986) and *T. pseudonana* (Cullen and Lewis 1988) and a Chl : L ratio for L of 0.2, we calculate $\kappa_L = \theta_{max}/\text{Chl} : \text{L} = 0.4$.

Maintenance metabolic rate constant—r_m can be estimated by extrapolation of respiration rate to $\mu = 0$. This exercise typically yields values for r_m of <0.1 d^{-1} (Geider 1992), consistent with the low rate of protein turnover observed in nutrient replete *Chlorella fusca* (Richards and Thurston 1980)—the only microalgae for which reliable data are available. A low value for r_m is also consistent with low rates of pigment turnover obtained from ^{14}C-labeling experiments (Goericke and Welschmeyer 1992). We have chosen a value of 0.05 d^{-1}. For diatoms, which

typically have high light-saturated growth rates, the respiration term in our model becomes significant only at extremely low irradiances under conditions of balanced growth. Thus, the choice of r_m values is not critical. The value chosen for r_m may be more critical for modeling slowly growing phytoplankters. Parameterization of respiration as a constant—independent of previous environmental conditions—may affect the fidelity of the model during transients following a shift-down of irradiance. This point is addressed in the discussion.

The maximum rate of photosynthesis—The value of P^E_m is intrinsically linked to the resource-saturated maximum growth rate. At maximum growth rate, Eq. 6 becomes

$$\mu_m = \frac{1}{C}\frac{dC}{dt} = P^E_m \frac{E}{C} - r_m. \quad (8)$$

Rearranging, we obtain

$$P^E_m = (\mu_m + r_m)\frac{C}{E} = \frac{(\mu_m + r_m)}{\kappa_E}. \quad (9)$$

In words, P^E_m can be determined from the maximum growth rate, the maintenance metabolic rate, and the ratio of C:E. the model requires that $C:E = 1/\kappa_E$ under all conditions, as inspection of Eq. 2–5 will verify. Since we have already determined that $\kappa_L = 0.4$ and thus that $\kappa_E = (1 - \kappa_L) = 0.6$, it follows that $P^E_m = 1.66\ (\mu_m + r_m)$.

The parameter values used in a simulation must be tailored to the species under consideration. However, it is important to recognize that the parameters are not strictly independent. Changing the value of the relative maximum size of L (κ_L) has implications for the derived value of P^E_m if μ_m is constant. Similarly, changing the value of κ_L will affect the value of the functional cross-section (σ) if Chl:L and θ_{max} are constant. Laboratory observations have demonstrated that a^*_{Chl} can vary by a factor of three within and between species (Falkowski et al. 1985) and that μ_m can vary from <0.5 to >3 d^{-1} among species and with temperature (Eppley 1972). Clearly, the assumption of constant σ is inconsistent with variability of a^*_{Chl} unless there are compensating changes of ϕ_m, as is commonly observed (Geider 1993). Variations in the measured variables a^*_{Chl} and μ_m can arise from differences in the allocation of resources to L and E among species (i.e. from a change in κ_L and κ_E) at fixed σ and P^E_m, from variations in the catalytic efficiencies σ and P^E_m (at fixed κ_L), or from some combination of effects. Observations of growth rate and Chl *a*:protein ratios in diatoms and dinoflagellates are consistent with compensatory changes in resource allocation and catalytic efficiencies (Chan 1978).

Balanced growth: Comparison of predictions with observations—The model can be solved analytically for balanced growth (Geider et al. in prep.) to yield the following expressions for the light dependence of θ and μ:

Table 1. Parameter values used to model steady-state, nutrient-saturated growth of *Thalassiosira pseudonana* and *Phaeodactylum tricornutum*.

Parameter	*T. pseudonana*	*P. tricornutum*	Dimensions
σ	2.0	1.0	$m^2\ mol^{-1}$ photons
κ_L	0.4	0.4	Dimensionless
κ_E	0.6	0.6	Dimensionless
Chl:L	0.2	0.2	g Chl *a* g^{-1} C
P^E_m	5.55	2.4	d^{-1}
r_m	0.05	0.05	d^{-1}

$$\theta = \theta_{max}\left[\frac{1}{1 + (\theta_{max}\alpha I)/(2P^C_m)}\right] \quad (10)$$

$$\mu = P^C_m[1 - \exp(-\alpha I\theta/P^C_m)] - r_m. \quad (11)$$

P^C_m is the C-specific light-saturated photosynthesis rate, $P^C_m = (P^E_m\ E)/C = \mu_m + r_m$, and α is the Chl *a*-specific initial slope of the *PI* curve. Note that the irradiance dependence of θ can be predicted by specifying the values of three parameters. The value of θ calculated from Eq. 10 can be inserted into Eq. 11 to calculate the growth rate, provided that the respiration rate is also known. For completeness, we have presented the analytical solutions (Eq. 10 and 11) without derivation. The derivation and further discussion of the application of these equations is provided by Geider et al. (in prep.).

The model predictions were compared with observations for the diatoms *P. tricornutum* (Geider et al. 1985, 1986) and *T. pseudonana* (Cullen and Lewis 1988). Using the parameter values given in Table 1, we obtained good agreement between predicted and observed growth rate (μ) and pigment content (θ). The balanced growth rate is a saturating function of irradiance (Fig. 3A, B). To account for the differences in growth rate between *P. tricornutum* and *T. pseudonana,* we needed to specify different values of σ and P^E_m for the two species. Although the difference in μ_m is real, it remains to be determined whether the variation in σ between these diatoms is due to interspecific differences in light absorption and energy conversion or to the differences in light sources and optical geometries used by Geider et al. (1985, 1986) and Cullen and Lewis (1988). Maximum values of θ are observed at low light-limiting irradiances, with a sigmoidal decrease of θ as $\log(I)$ increases (Fig. 3C, D). Both species appear to be characterized by similar values of θ_{max}.

Recent observations of regulation of photoadaptation in the chlorophyte *D. tertiolecta* bear on our parameterization of regulation by the term $(P^E E)/(\sigma I L)$. Escoubas et al. (1995) demonstrated that the redox state of the plastoquinone pool provides the signal regulating photoadaptation in *D. tertiolecta.* Following a shift from low- to high-light conditions, the plastoquinone pool is highly reduced, the synthesis of mRNA encoding the light-harvesting complex proteins (*cab* mRNA) declines, and *D. tertiolecta* adapts by reducing the rate of synthesis of light-harvesting complex proteins. In contrast, following a shift

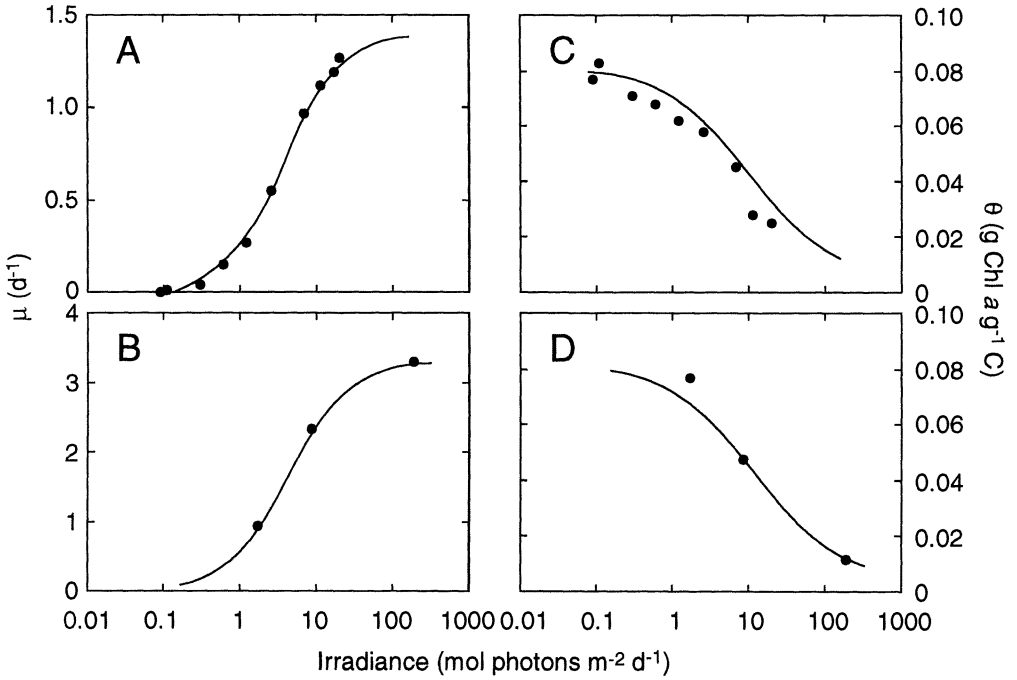

Fig. 3. Observed (●) and predicted (——) dependencies of growth rate (μ) and the Chl *a*: C ratio (θ) on irradiance of fully acclimated *Phaeodactylum tricornutum* (A and C) and *Thalassiosira pseudonana* (B and D). Observations are from Geider et al. (1985, 1986) and Cullen and Lewis (1988). Values for the model parameters used to obtain the predicted relations are given in Table 1.

from high- to low-light conditions, the plastoquinone pool is highly oxidized, *cab* mRNA synthesis is enhanced, and the rate of synthesis of light-harvesting complex protein is also enhanced following a lag during which *cab* mRNA accumulates (Escoubas et al. 1995). One of the assumptions of our model is that the variation of θ with irradiance provides an index of the down-regulation of the rate of synthesis of L. Under conditions of balanced growth, our model requires that $\theta = \theta_m (P^E E)/(\sigma I L)$. We anticipate that in the steady state, the oxidation-reduction status of the plastoquinone pool should parallel changes of θ. Specifically, the plastoquinone pool should be more reduced at high irradiance, and θ should decline in parallel with the proportion of plastoquinone that is in the reduced form, although the relationship need not be linear. Using the recently developed fast-repetition-rate fluorescence technique to assess the redox state of plastoquinone pool (Prasil et al. in prep.) will allow this assumption to be tested.

Dynamics of photoadaptation: Comparison of prediction with observation

The agreement of predicted and observed values of μ and θ in nutrient-saturated cultures maintained in balanced growth at a range of irradiances (Fig. 3) shows that the model captures essential features of photoadaptation. A more rigorous test of the dynamic model is the ability to predict changes of pigment and carbon content of cultures following changes of irradiance. Observations of particulate C and Chl *a* for *T. pseudonana* during reciprocal step shifts in growth irradiance (Cullen and Lewis 1988) allow this comparison to be made. The parameter values given in Table 1 were used in Eq. 2–5 to predict changes of θ and the concentrations of carbon [C] and chlorophyll *a* [Chl *a*] for cultures of *T. pseudonana* subjected to irradiance shifts between 8.6 and 190 mol photons m^{-2} d^{-1} (100 and 2,200 μmol photons m^{-2} s^{-1}). The dynamic model predicts the general shape of the responses of θ during the transients following reciprocal shifts of irradiance (Fig. 4A). However, examination of the predicted and observed variations of [Chl *a*] and [C] show a divergence of prediction from observation (Fig. 4B and C). The divergence is greater for the step-down (Fig. 4C) than the step-up (Fig. 4B) in irradiance. Specifically, predicted Chl *a* and C accumulation rates are much greater than observed rates following the shift-down of irradiance.

A possible explanation for the divergence between predictions and observations is that phytoplankton possess photoprotective mechanisms that are not included in the model. These mechanisms could serve to modify σ by affecting ϕ_m, thus altering the ratio $(P^E E):(\sigma I L)$ in ways not accounted for by our model. Reversible changes in the functional cross-section of photosystem 2 associated with xanthophyll cycle activity (Olaizola et al. 1994) will modify the regulatory term $(P^E E)/(\sigma I P)$ and the photosynthesis rate. In addition, accumulation of photoinhibitory damage could account for a decrease in the rate of C fixation in cells shifted to very high irradiance but not predicted by the model. These explanations are not ap-

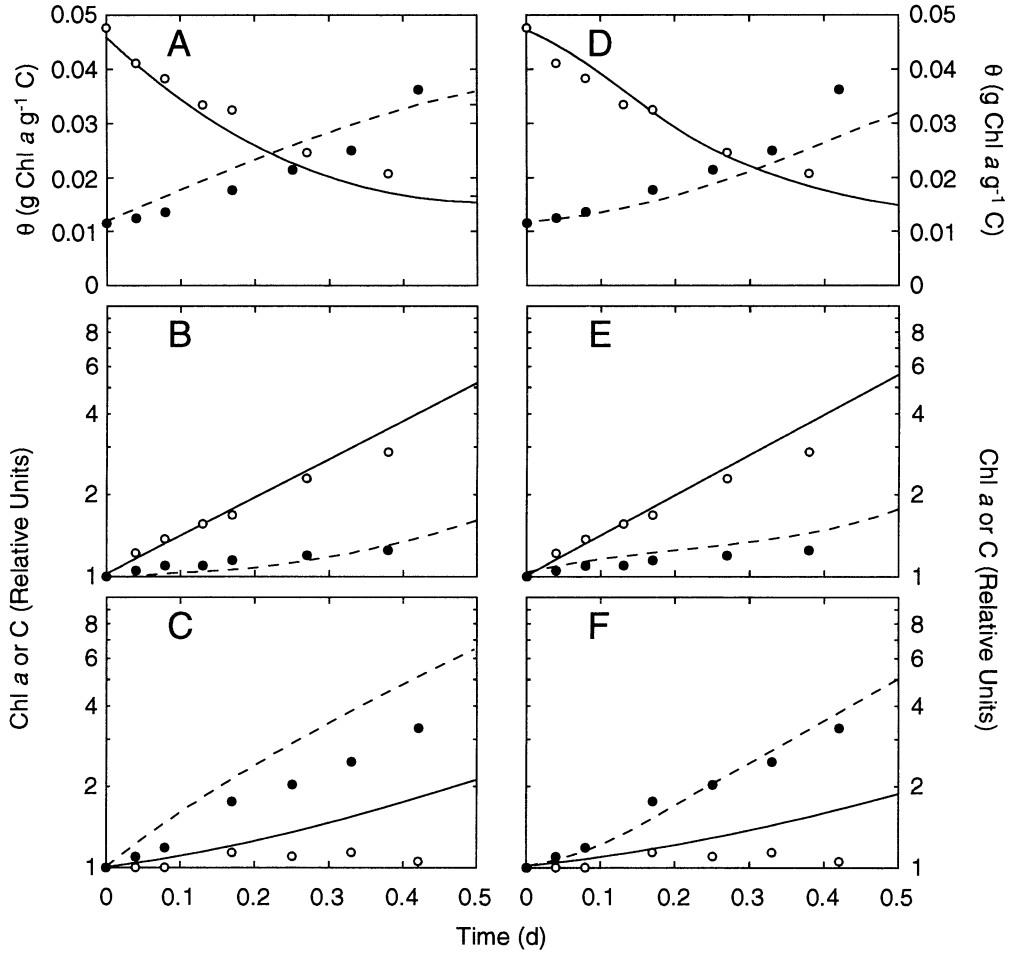

Fig. 4. Observed and predicted changes of θ and of [Chl *a*] and [C] in *Thalassiosira pseudonana* during light shift experiments (observations of Cullen and Lewis 1988). A. Changes of θ during reciprocal shifts between irradiances of 8.6 and 190 mol photons m^{-2} d^{-1} continuous illumination. The predicted changes are based on Eq. 2–5 using the parameter values given in Table 1. Shift-up (○,——) and shift-down (●,– – –) are indicated. B. Relative changes of [Chl *a*] (●,– – –) and [C] (○,) during a shift-up of irradiance from 8.6 to 190 mol photons m^{-2} s^{-1}. Predictions are based on Eq. 2–5. Data are expressed relative to the initial values. C. Relative changes of [Chl *a*] and [C] during the shift-down from 190 to 8.6 mol photons m^{-2} s^{-1} (symbols as in panel B). Predictions are based on Eq. 2–5. Note that the predicted increase of Chl *a* is much more rapid than the observed increase. D. Changes of θ during reciprocal shifts of irradiance (symbols as in panel A). The observations are as in panel A, and the predictions are based on the time-lagged model (Eq. 2–4 and 10–13). E. Relative changes of Chl *a* and C during a shift-up (symbols as in panel B). The observations are as a panel B, and the predictions are based on the time-lagged model. F. Relative changes of Chl *a* and C during a shift-down in irradiance. The observations are as in panel C, and the predictions are based on the time-lagged model.

plicable to the observations presented in Fig. 4 for *T. pseudonana* (*see* Lewis et al. 1984*a*), so we need to look elsewhere for an explanation of the divergence between prediction and observation.

Coupling of information to material fluxes

The dynamic model assumes that the allocation of photosynthate to L and R responds instantaneously to changes of irradiance through a change in the ratio of photosynthesis to light absorption [i.e. $(P^{E}E)/(\sigma IL)$]. This assumption does not affect the solution of the model under conditions of balanced growth. However, an explanation for the deviation of observed and predicted behavior illustrated in Fig. 4A, B, and C could arise from a limitation imposed on the dynamic model by this assumption. It is likely that signal transduction, resulting in a decline of pigment synthesis in high light or enhanced pigment synthesis in low light, operates with an intrinsic lag. One can hypothesize that the lag is associated with changes in the level of molecule signaling synthesis of light-harvesting

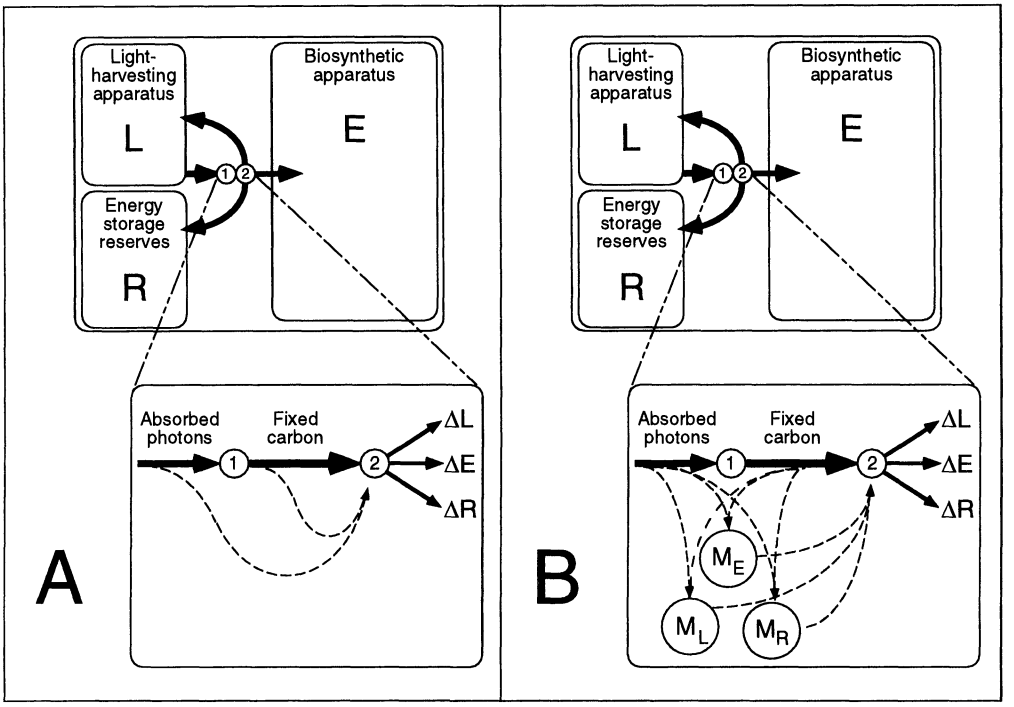

Fig. 5. Diagrammatic illustration of the coupling of signal transduction to biosynthesis during photoadaptation. Flows of energy and fixed C are illustrated by solid arrows; signal transduction is illustrated by dashed arrows. The signal mediating photoadaptation is determined by the ratio of the rate of C fixation to the rate of photon absorption as parameterized by $(P^{E}E)/(\sigma I L)$. (*See text for details.*) Panel A illustrates the instantaneous response, in which the redox state of a component of the photosynthetic electron transfer directly regulates the allocation of fixed C between synthesis of new L (ΔL), new E (ΔE), or R (ΔR). Panel B illustrates the role of signal pools (M_E, M_L, and M_R) in mediating signal transduction. The allocation of photosynthate among ΔL, ΔE, and ΔR is assumed to be proportional to the abundances of M_L, M_E, and M_R as described in the text. Thus, a time lag is introduced into the response.

complex proteins. This molecule could be mRNA for light-harvesting complex proteins. La Roche et al. (1991) and Escoubas et al. (1995) have shown that mRNA encoding the light-harvesting complex proteins of *D. teriolecta* increases following a shift from high to low irradiance.

To examine the consequences of this hypothesis, we formulated a model of information flow to drive the allocation of photosynthate in the dynamic model. We assume that the rate of synthesis of each of the three components of the model phytoplankter (L, E, and R) is determined by a strict competition among signals coding for these components. To avoid unwarranted precision, we prefer to frame the model in terms of somewhat ill-defined "signals" rather than precisely defined mRNAs; however, we assume that the signals of our model are in many respects analogous to mRNA levels. We recognize that this assumption of strict regulation of relative rates of protein synthesis by mRNA pool sizes is not generally applicable. For example, chloroplast-encoded proteins show high degrees of translational control (Harris et al. 1994). However, the translational control of chloroplast-encoded protein synthesis is exerted, at least in part, by nuclear-encoded proteins that must be synthesized and degraded-sequestered in order to regulate protein synthesis. Thus, the signals may be pools of regulatory proteins rather than pools of mRNA.

Designating the signal levels for L, E, and R as M_L, M_E, and M_R, we require that

$$\rho_L = M_L/M_T; \qquad \rho_E = M_E/M_T; \qquad \rho_R = M_R/M_T \quad (12)$$

where $M_T = M_L + M_E + M_R$. We assume that the relative rates of M_L and M_R synthesis are determined by the regulatory term $(P^{E}E)/(\sigma I L)$ as depicted in Eq. 13–15. We recognize that this treatment is grossly oversimplified. However, it is a convenient approach for introducing a time lag into information flow and cellular responses.

Conceptual diagrams depicting the models of instantaneous and lagged responses in allocation of photosynthate among intracellular pools (i.e. changes of ρ_L and ρ_R) are illustrated in Fig. 5. There are two control points in these diagrams. A signal is generated by comparing fluxes around the first control point. This signal is the imbalance between photon absorption and carbon fixation specified as $(P^{E}E)/(\sigma I L)$. The allocation of resources between L, E, and R occurs at a second control point. For the instantaneous response, synthesis rates of L, E, and R respond directly to imbalances in the ratio of light absorption to C fixation (Fig. 5A). A lag is introduced when the signal operates by modifying the relative concentrations of three

signal pools (Fig. 5B) which in turn influence the relative rates of synthesis of L, E, and R.

The problem now becomes one of specifying the dynamics controlling the signal levels M_L, M_E, and M_R. We start with the requirement that Eq. 12 giving the values of ρ_L, ρ_E, and ρ_R be identical to Eq. 5 for steady-state (i.e. balanced) growth. This limits the possible choices of the dynamic equations describing change of M_L, M_E, and M_R and ensures that the regulatory term $(P^E E)/(\sigma I L)$ appears in the equations describing changes of M_L and M_R. The changes in M_L, M_E, and M_R can result from changes in the rates of synthesis and degradation of signal (Fig. 6). There is strong evidence for light regulation of the rate of transcription of mRNAs coding for light harvesting complex in higher plants and microalgae (La Roche et al. 1991; Escoubas et al. 1995). An increase in the rate of transcription (synthesis of M_L) can adequately account for the delay in net Chl *a* synthesis during a shift from high to low irradiance. In our formulation of signal transduction, the nearly immediate cessation of net Chl *a* accumulation upon a transfer from low to high irradiance requires that the stability of M_L decrease in high light. It is possible, however, that other mechanisms can account for a change in net pigment accumulation. These include down-regulation of pigment synthesis (Thompson and White 1991) or enhanced pigment turnover (Riper et al. 1979). Chlorophyll synthesis has been shown to be essential for accumulation of pigment protein complexes in *D. tertiolecta* (Mortain-Bertrand et al. 1990). We have assumed that the down-regulation of synthesis of light-harvesting complex proteins (and associated pigments) occurring in response to increased irradiance is mediated by changing sizes of signal pools. We recognize that experimental work is required to establish the relative importance of decreased signal stability, increased pigment turnover, and regulation of pigment synthesis (as related to regulation of light-harvesting protein synthesis) during adaptation to high light.

We attempted a number of different formulations of the regulation of M_L synthesis and degradation and settled on a formulation in which both down-regulation of synthesis of M_L and increased degradation of M_L occur in response to increased irradiance. We chose this formulation because assigning all of the regulation to control of M_L and M_R synthesis resulted in a significant overestimate of Chl *a* concentrations from the observation during the shift-up. The regulatory term $(P^E E)/(\sigma I L)$ is thus split between effects on synthesis and degradation of M_L. The sizes of the signal pools are assumed to change with variations in the rates of signal synthesis and turnover as follows:

$$\frac{dM_L}{dt} = k_L[(P^E E)/(\sigma I L)]^{1/2} - \frac{k_t M_L}{[(P^E E)/(\sigma I L)]^{1/2}}, \quad (13)$$

$$\frac{dM_R}{dt} = k_L[1 - [(P^E E)/(\sigma I L)]^{1/2} - \frac{k_t M_R}{1 - [(P^E E)/(\sigma I L)]^{1/2}}, \quad (14)$$

and

$$\frac{dM_E}{dt} = k_E - k_t M_E. \quad (15)$$

k_L is the maximum rate of M_L or M_R synthesis, k_E is the maximum rate of M_E synthesis, and k_t is the signal degradation time constant. We assume that $k_L = k_t \kappa_L$ and $k_E = k_t \kappa_E$. In Eq. 13, $[(P^E E)/(\sigma I L)]^{1/2}$ is multiplied by k_L to account for the down-regulation of synthesis of M_L, and $k_t M_L$ is divided by $[(P^E E)/(\sigma I L)]^{1/2}$ to account for an increased degradation rate at high irradiance.

Solving Eq. 13–15 for steady-state signal levels [i.e. $(1/M)(dM/dt) = 0$], we obtain the values of ρ_L, ρ_E, and ρ_R given in Eq. 5. Thus, the steady-state solution of a model specifying signal levels by Eq. 12–15 is identical to the solution of the original dynamic model (Eq. 2–5). However, the predicted transient behavior changes significantly. We assumed arbitrarily that $k_t = 5\ d^{-1}$, consistent with complex light-harvesting proteins of *D. tertiolecta* (Escoubas et al. 1995). Substituting the values obtained from Eq. 12 to 15 into the dynamic model (Eq. 2–4) yields predictions of the transient behavior following step changes of irradiance illustrated in Fig. 4D, E, F. Changes of [Chl *a*], [*C*], and θ during the high to low shift occur more slowly when a time lag for information flow is incorporated into the dynamic model, and the predictions agree more closely to observations (Fig. 4D, E, F). Pigment synthesis continues for a short time following the shift from low to high light, although the model slightly overestimates this effect (Fig. 4E). Inspection of all of the data provided by Cullen and Lewis (1988) suggests that Chl *a* synthesis stops abruptly following the low- to high-light shift.

The effect of varying the signal synthesis and turnover rate constants on the proportion of photosynthate directed to biosynthesis of L (i.e. $\rho_L = M_L/M_T$) is illustrated in Fig. 7. The decline of ρ_L following a shift-up in irradiance is rapid, approaching a step change. However, there is a small undershoot in ρ_L relative to the new steady-state value (Fig. 7A). In contrast, the rate of increase of ρ_L following a step-down in irradiance is much slower (Fig. 7B) and cannot be readily accommodated by the simpler model that assumes instantaneous up-regulation of synthesis of L upon a shift from high to low irradiance. Equations 13–15 predict an overshoot in ρ_L that is consistent with observations of mRNA levels for light-harvesting complex proteins in *D. tertiolecta* following a shift-down in irradiance (La Roche et al. 1991). The predicted asymmetry in the response of ρ_L to increased and decreased irradiance may have significant implications for phytoplankton growth and photoadaptation in the surface mixed layer. Specifically, the model predicts that adaptation to high light will be much more rapid than adaptation to low light. In addition, brief exposures to high irradiance will outweight much longer exposures to low irradiance in determining the photoadaptive state of the phytoplankton. This prediction of the model is consistent with observations that phytoplankton seem to be adapted to the highest irradiances experienced as they cycle through the mixed layer rather than to the average irradiance within the mixed layer (Vincent et al. 1994). In contrast, Cul-

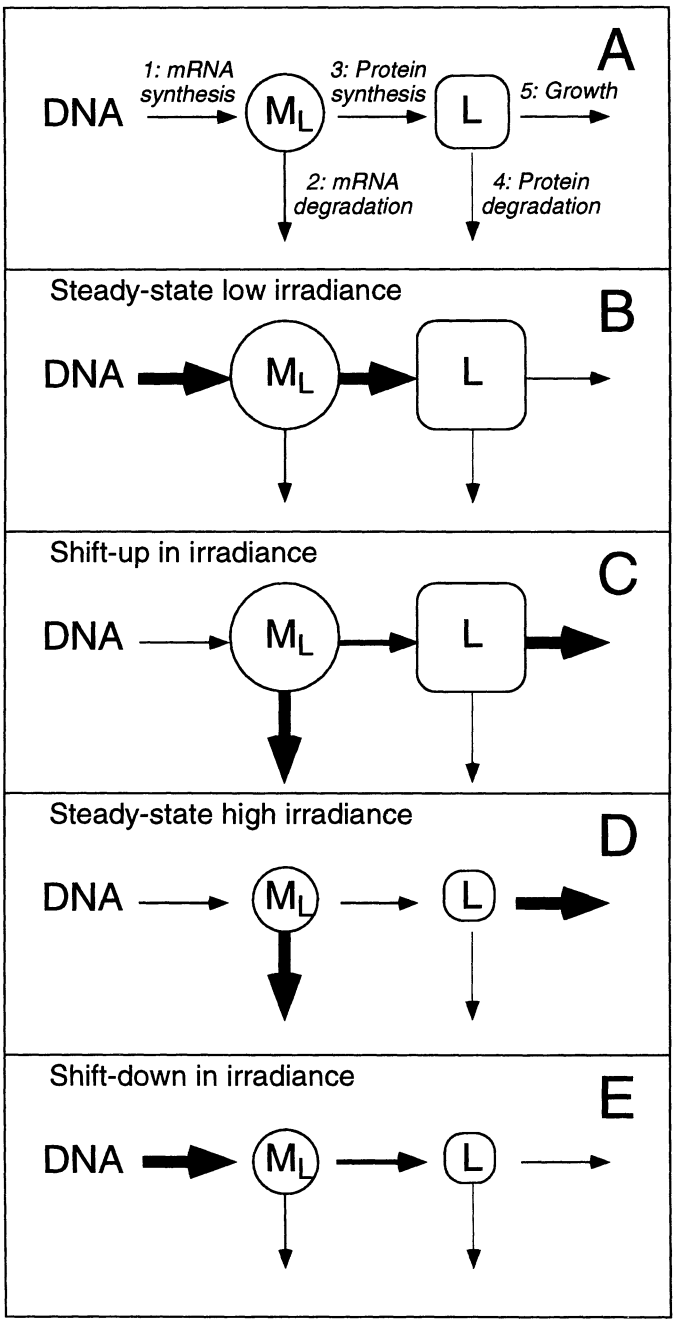

Fig. 6. Diagrams indicating coupling of information flow to protein synthesis and growth. A. Arrows indicate rate constants, and arrow thickness represents the magnitudes of the rate constants. The size of the signal pool for M_L, as a proportion of total signal, varied in response to changes in the rates of signal synthesis and degradation. The proportion of cell C in L changes as a result of protein synthesis and degradation. B. The steady-state low light condition in which a high rate constant for M_L synthesis and low constant for M_L degradation results in a large pool of M_L. This in turn stimulates allocation of a large proportion of photosynthate to synthesis of L. Growth is low, however, because irradiance limits photosynthesis. C. A decrease in the rate constant for M_L synthesis and increase in the rate constant for M_L degradation occur immediately after an increase of irradiance. However, synthesis of L continues at a high rate until the M_L pool is drained. The decline of M_L can be quite rapid (*see Fig. 7A*). D. The steady-state high light condition in which M_L is maintained at a low level by a low rate constant for synthesis and high rate constant for degradation. The rate constant for growth is high, however, because photosynthesis is light saturated. E. The rate constant for M_L synthesis increases and the constant for M_L degradation decreases immediately after a shift-down of irradiance. However, a delay arises before synthesis of L reaches the new steady-state level because of the need for M_L to increase (Fig. 7B).

len and Lewis (1988) concluded that adaptation to low light was more rapid than adaptation to high light.

Mobilization of the energy reserve pool, respiration, and the cost of biosynthesis

Our model focuses on regulation of pigment synthesis during photoadaptation. Respiration is simply treated as a constant and small maintenance metabolic rate. However, it is likely that variations in the respiration rate associated with pigment and protein turnover and with mobilization of energy storage reserves will be a significant component of the response to a change in environmental conditions. In fact, examination of Fig. 4C and F shows zero net organic C accumulation in the culture shifted from high to low light, indicating that gross photosynthesis is balanced by respiration in this experiment. Thus, one of the major limitations of the dynamic model as formulated in Eq. 2–4 is failure to include mobilization of the energy reserve pool. An increase in respiration not accommodated by our model accounts for at least part of the divergence of observed [C] from predictions in the irradiance step-down experiment (Fig. 3C, F). Energy reserves are known to be mobilized in darkness to support continued synthesis of macromolecules (Foy and Smith 1980; Cuhel et al. 1984; Lancelot and Mathot 1985). However, the respiration of organic carbon to CO_2 will be substantially less than the rate of mobilization of carbohydrate. Despite mobilization of carbohydrates and lipids during darkness, Falkowski and La Roche (1991) concluded that phytoplankton do not acclimate to shade at night, indicating that the signal regulating photoadaptation is preserved during the dark period.

Variations in the rate of turnover of macromolecules may play a role in photoadaptation following changes in environmental conditions. Protein turnover is difficult to detect in exponentially growing microalgae (Richards and Thurston 1980), consistent with the low maintenance metabolic rate of microalgae (Geider 1992). There are conflicting reports on the magnitude of chlorophyll *a* turnover in microalgae (Riper et al. 1979; Goericke and Welschmeyer 1992). Even if low rates of pigment turnover under conditions of balanced growth are the rule (Goericke and Welschmeyer 1992), pigment degradation may be accelerated during transients following increases in irradiance or decreases in nutrient supply. Protein turnover also increases to a rate as high as 0.7 d^{-1} during unbalanced growth when *Chlorella* sp. enters stationary

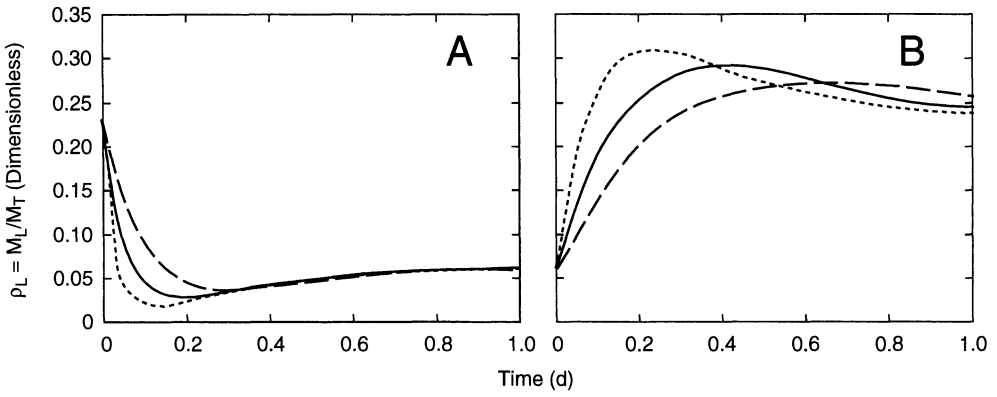

Fig. 7. Predicted changes in $M_L : M_T = \rho_L$ during (A) the shift-up from 8.6 to 190 mol photons m^{-2} s^{-1} and (b) the reciprocal shift-down. Solid curves show changes of ρ_L corresponding to the stimulation illustrated in Fig. 3D, E, and F in which $k_L = 2$ d^{-1}, $k_E = 3$ d^{-1}, and $k_t = 5$ d^{-1}. Dotted curves indicate the changes of ρ_L for 2-fold greater values of K_L, k_E, and k_t; dashed curves indicate the changes of ρ_L for 2-fold lower changes of k_L, k_E, and k_t.

phase (Richards and Thurston 1980). The constancy of chlorophyll *a* concentration in *T. pseudonana* following a shift-up in irradiance observed by Cullen and Lewis (1988) (Fig. 4C) could arise from a balance between synthesis and degradation of chlorophyll *a* or from a rapid decline in the gross rate of pigment synthesis following the shift-up in irradiance.

Conclusions and future research

A simple dynamic model of photoadaptation incorporating material fluxes and an explicit description of regulation of pigment synthesis (Eq. 2–5) can describe essential features of phytoplankton growth and photoadaptation in constant and fluctuating light. Consideration of time lags in information transduction (Eq. 12–15) in the dynamic model improves prediction of photoadaptation of pigment content following step changes of irradiance. One consequence of our formulation of photosynthesis (Eq. 1) and resource allocation (Eq. 2–5) is an ability to account for lagged responses (i.e. the "memory" of past environmental conditions, such as described by Jones 1978). In addition, explicit consideration of regulation may allow incorporation of other signals, such as circadian rhythms (Ernst et al. 1990), by specifying their effects on modulating rates of pigment and protein synthesis. The model provides a formal strategy for quantitatively relating the molecular mechanisms of photoadaptation to the ecophysiological responses. Although capable of accounting for observed photoadaptation of pigment content and growth rate, the model has not been rigorously tested and remains largely heuristic. Rigorous testing is feasible because the model specifies that photoadaptation results from changes in the rates of macromolecule synthesis and degradation, with synthesis regulated by resource availability (i.e. light and information flow, *see Fig. 6*). The regulatory component is based on changing signal levels.

There are many limitations in our dynamic model that can only be redressed by focused experimental research. Among the areas that need to be addressed are the rules governing the mobilization of energy reserve polymers, the importance of photoinhibition in high light adaptation, nutrient uptake and limitation, the role of turnover (i.e. controlled degradation) of key macromolecules, the signal transduction pathways modulating the synthesis of key macromolecules, and the modulation of catalytic efficiencies that occur independently of net pigment and protein synthesis. Despite these limitations, the model provides insights into the basic mechanism of photoadaptation and a link between molecular, physiological, and ecological aspects of phytoplankton biology.

Photoadaptation is a universal feature of algal physiology. Although there are many descriptions of photoadaptation in laboratory and natural phytoplankton populations, there have been few attempts to calculate the change in fitness that accompanies photoadaptation. Ultimately, the success of a phytoplankton population in nature depends on achieving a positive balance between cell division and death. Photoadaptation presumably enhances cell division; as such, it should contribute to the positive side of this balance. We anticipate that explicit consideration of physiological adaptation within the context of ecosystem models of planktonic food webs will allow us to address the relative importance of physiological responses vs. predation and physical transport on phytoplankton population dynamics and productivity.

References

CHAN, A. T. 1978. Comparative physiological study of marine diatoms and dinoflagellates in relation to irradiance and cell size. 1. Growth under continuous light. J. Phycol. **14:** 396–402.

CUHEL, R. L., P. B. ORTNER, AND D. R. S. LEAN. 1984. Night synthesis of protein by algae. Limnol. Oceanogr. **29:** 731–744.

CULLEN, J. J. 1982. The deep chlorophyll maximum layer: Comparing vertical profiles of chlorophyll *a*. Can. J. Fish. Aquat. Sci. **39:** 791–803.

———, AND OTHERS. 1993. Toward a general model of phy-

toplankton growth for biogeochemical models, p. 153–176. *In* G. T. Evans and M. J. R. Fasham [eds.], Towards a model of ocean biogeochemical processes. Springer.

———, AND M. R. LEWIS. 1988. The kinetics of algal photoadaptation in the context of vertical mixing. J. Plankton Res. **10:** 1039–1063.

EPPLEY, R. W. 1972. Temperature and phytoplankton growth in the sea. Fish. Bull. **70:** 1063–1085.

ERICKSON, J. M., AND J.-D. ROUCHAIX. 1992. The molecular biology of photosystem 2, p. 101–178. *In* J. Barber [ed.], The photosystems: Structure, function and molecular biology. Elsevier.

ERNST, D., A. APFELBÖCK, A. BERGMANN, AND C. WEYRAUCH. 1990. Rhythmic regulation of the light-harvesting chlorophyll *a/b* protein and the small subunit of ribulose-1,5-bisphosphate carboxylase mRNA in rye seedlings. Photochem. Photobiol. **52:** 29–33.

ESCOUBAS, J.-M., M. LOMAS, J. LAROCHE, AND P. G. FALKOWSKI. 1995. Light intensity regulation of calogene transcription is signaled by the redox state of the plastoguinone pool. Proc. Natl. Acad. Sci. **92:** 10,237–10,241.

FALKOWSKI, P. G., Z. DUBINSKY, AND K. WYMAN. 1985. Growth-irradiance relationships in phytoplankton. Limnol. Oceanogr. **30:** 311–321.

———, AND J. LA ROCHE. 1991. Acclimation to spectral irradiance in algae. J. Phycol. **27:** 8–14.

———, AND T. G. OWENS. 1980. Light-shade adaptation: Two strategies in marine phytoplankton. Plant Physiol. **66:** 592–595.

FISHER, T., R. SHURTZ-SWIRSKI, S. GEPSTEIN, AND Z. DUBINSKY. 1989. Changes in the levels of ribolose-1,5-bisphosphate carboxylase/oxygenase (Rubisco) in *Tetraedron minimum* (Chlorophyta) during light and shade adaptation. Plant Cell Physiol. **30:** 221–228.

FOY, R. H., AND R. V. SMITH. 1980. The role of carbohydrate accumulation in the growth of planktonic *Oscillatoria* species. Br. Phycol. J. **15:** 139–150.

FRIEDMAN, A. L., AND R. S. ALBERTE. 1984. A diatom light-harvesting pigment-protein complex: Purification and characterization. Plant Physiol. **76:** 483–489.

GALLEGOES, C. L., AND T. PLATT. 1985. Vertical advection of phytoplankton and productivity estimates: A dimensional analysis. Mar. Ecol. Prog. Ser. **26:** 125–134.

GEIDER, R. J. 1984. Light and nutrient effects on algal physiology. Ph.D. thesis, Dalhousie Univ. 187 p.

———. 1987. Light and temperature dependence of the carbon : chlorophyll *a* ratio in microalgae and cyanobacteria: Implications for physiology and growth of phytoplankton. New Phytol. **106:** 1–34.

———. 1992. Respiration: Taxation without representation, p. 333–360. *In* P. G. Falkowski [ed.], Primary productivity and geochemical cycles in the sea. Plenum.

———. 1993. Quantitative phytoplankton ecophysiology: Implications for primary production and phytoplankton growth. ICES Mar. Sci. Symp. 197, p. 52–62.

———, B. A. OSBORNE, AND J. A. RAVEN. 1985. Light dependence of growth and photosynthesis in *Phaeodactylum tricornutum* (Bacillariophyceae). J. Phycol. **21:** 609–619.

———, ———, AND ———. 1986. Growth, photosynthesis and maintenance metabolic cost in the diatom *Phaeodactylum tricornutum* at very low light levels. J. Phycol. **22:** 39–48.

———, AND T. PLATT. 1986. A mechanistic model of photoadaptation in microalgae. Mar. Ecol. Prog. Ser. **30:** 85–92.

GOERICKE, R., AND N. A. WELSCHMEYER. 1992. Pigment turnover in the marine diatom *Thalassiosira weissflogii*. 1. The $^{14}CO_2$-labeling kinetics of chlorophyll *a*. J. Phycol. **28:** 498–507.

HARRIS, E. H., J. E. BOYNTON, AND N. W. GILHAM. 1994. Chloroplast ribosomes and protein synthesis. Microbiol. Rev. **58:** 700–754.

HARRISON, W. G., AND T. PLATT. 1986. Photosynthesis-irradiance relationships in polar and temperate phytoplankton populations. Polar Biol. **5:** 153–164.

HOPE, A. B. 1993. The chloroplast bf complex: A critical focus on function. Biochim. Biophys. Acta **1143:** 1–22.

IKEUCHI, M. 1992. Subunit protein of photosystem 1. Plant Cell Physiol. **3:** 669–676.

JONES, R. I. 1978. Adaptations to fluctuating irradiance by natural phytoplankton communities. Limnol. Oceanogr. **23:** 920–926.

KAMYKOWSKI, D., H. YAMAZAKI, AND G. S. JANOWITZ. 1994. A Lagrangian model of phytoplankton photosynthetic response in the upper mixed layer. J. Plankton Res. **16:** 1059–1069.

KANA, T. M., AND P. M. GLIBERT. 1987. Effect of irradiances up to 2000 μE m^{-2} s^{-1} on marine *Synechococcus* WH7803. 2. Photosynthetic responses and mechanisms. Deep-Sea Res. **34:** 497–516.

LANCELOT, C., AND S. MATHOT. 1985. Biochemical fractionation of primary production by phytoplankton in Belgian coastal waters during short- and long-term incubations with ^{14}C-bicarbonate. 1. Mixed diatom population. Mar. Biol. **86:** 219–226.

———, C. VETH, AND S. MATHOT. 1991. Modelling ice-edge phytoplankton bloom in the Scotia-Weddel Sea sector of the Southern Ocean during Spring 1988. J. Mar. Syst. **2:** 333–346.

LANGDON, C. 1988. On the causes of interspecific differences in the growth-irradiance relationship for phytoplankton. 2. A general review. J. Plankton Res. **10:** 1291–1312.

LA ROCHE, J., A. MORTAIN-BERTRAND, AND P. G. FALKOWSKI. 1991. Light intensity-induced changes in cab mRNA and light harvesting complex 2 apoprotein levels in the unicellular chlorophyte *Dunaliella tertiolecta*. Plant Physiol. **97:** 147–153.

LAWS, E. A., D. G. REDALJE, D. M. KARL, AND M. S. CHALUP. 1983. A theoretical and experimental examination of the predictions of two recent models of phytoplankton growth. J. Theor. Biol. **105:** 469–491.

LEWIS, M. R., J. J. CULLEN, AND T. PLATT. 1984*a*. Relationships between vertical mixing and photoadaptation of phytoplankton: Similarity criteria. Mar. Ecol. Prog. Ser. **15:** 141–149.

———, E. P. W. HORNE, J. J. CULLEN, N. S. OAKEY, AND T. PLAT. 1984*b*. Turbulent motions may control phytoplankton photosynthesis in the upper ocean. Nature **311:** 49–50.

LI, W. K. W., AND W. G. HARRISON. 1982. Carbon flow into the end-products of photosynthesis in short and long incubations of a natural phytoplankton population. Mar. Biol. **72:** 175–182.

———, AND T. PLATT. 1982. Distribution of carbon among photosynthetic end-products in phytoplankton of the eastern Canadian Arctic. J. Phycol. **18:** 466–471.

———, T. ZOHARY, Y. Z. YACOBI, AND A. M. WOOD. 1993. Ultraplankton in the eastern Mediterranean Sea: Towards deriving phytoplankton biomass from flow cytometric measurements of abundance, fluorescence and light scatter. Mar. Ecol. Prog. Ser. **102:** 79–87.

MARRA, J. 1978. Phytoplankton photosynthetic response to

vertical movement in a mixed layer. Mar. Biol. **46:** 203–208.

MITCHELL, B. G., AND D. A. KIEFER. 1988. Variability in pigment specific particulate fluorescence and absorption spectra in the northeastern Pacific Ocean. Deep-Sea Res. **35:** 665–689.

MIZIORKO, H. M., AND G. H. LORIMER. 1983. Ribulose-1,5-bisphosphate carboxylase-oxygenase. Annu. Rev. Biochem. **52:** 507–535.

MORRIS, I. 1981. Photosynthesis products, physiological state, and phytoplankton growth p. 83–102. *In* Physiological bases of phytoplankton ecology. Can. Bull. Fish. Aquat. Sci. **210.**

MORTAIN-BERTRAND, A., J. BENNETT, AND P. G. FALKOWSKI. 1990. Photoregulation of the light-harvesting chlorophyll protein complex associated with photosystem 2 in *Dunaliella tertiolecta.* Plant Physiol. **94:** 304–311.

OLAIZOLA, M., J. LA ROCHE, Z. KOLBER, AND P. G. FALKOWSKI. 1994. Non-photochemical fluorescence quenching and the diadinoxanthin cycle in a marine diatom. Photosyn. Res. **41:** 357–370.

ORELLANA, M. V., AND M. J. PERRY. 1992. An immunoprobe to measure Rubisco concentrations and maximal photosynthetic rates of individual phytoplankton cells. Limnol. Oceanogr. **37:** 978–990.

OWENS, T. G., AND E. R. WOLD. 1986. Light-harvesting function in the diatom *Phaeodactylum tricornutum.* 1. Isolation and characterization of pigment-protein complexes. Plant Physiol. **80:** 732–738.

RAVEN, J. A. 1984. A cost-benefit analysis of photo absorption by photosynthetic unicells. New Phytol. **98:** 593–625.

———, AND R. J. GEIDER. 1988. Temperature and algal growth. New Phytol. **110:** 441–461.

RICHARDS, L., AND C. F. THURSTON. 1980. Protein turnover in *Chlorella fusca* var. *vacuolata*: Measurement of the overall rate of intracellular protein degradation using isotope exchange with water. J. Gen. Microbiol. **121:** 49–61.

RIPER, P. M., T. G. OWENS, AND P. G FALKOWSKI. 1979. Chlorophyll turnover in *Skeletonema costatum,* a marine diatom. Plant Physiol. **64:** 49–54.

SAKSHAUG, E., K. ANDERSEN, AND D. A. KIEFER. 1989. A steady state description of growth and light absorption in the marine planktonic diatom *Skeletonema costatum.* Limnol. Oceanogr. **34:** 198–205.

SHUTER, B. 1979. A model of physiological adaptation in unicellular algae. J. Theor. Biol. **78:** 519–552.

SUKENIK, A., J. BENNETT, AND P. FALKOWSKI. 1987. Light-saturated photosynthesis—limitation by electron transport or carbon fixation? Biochim. Biophys. Acta **891:** 205–215.

THOMPSON, W. F., AND M. J. WHITE. 1991. Physiological and molecular studies of light-regulated nuclear genes in higher plants. Annu. Rev. Plant Physiol. Plant Mol. Biol. **42:** 423–466.

VINCENT, W. F., N. BERTRAND, AND J.-F. FRENETTE. 1994. Photoadaptation in intermittent light across the St. Lawrence estuary freshwater–saltwater transition zone. Mar. Ecol. Prog. Ser. **110:** 283–292.

WHITTMANN, H. G. 1982. Components of bacterial ribosomes. Annu. Rev. Biochem. **51:** 155–183.

Submitted: 14 November 1994
Accepted: 7 June 1995
Amended: 6 July 1995